High-field suppression of in-gap states in the Kondo insulator SmB_6

T. Caldwell,[1,2,*] A. P. Reyes,[1] W. G. Moulton,[1] P. L. Kuhns,[1] M. J. R. Hoch,[1] P. Schlottmann,[2] and Z. Fisk[2,†]
[1]*National High Magnetic Field Laboratory, Florida State University, Tallahassee, Florida 32310, USA*
[2]*Department of Physics, Florida State University, Tallahassee, Florida 32306, USA*
(Received 25 September 2006; published 12 February 2007)

The controversial ground-state properties of the Kondo insulator SmB_6 have been investigated using ^{11}B NMR in very high magnetic fields up to 37 T. We find evidence that, following the development of a gap in the conduction-band density of states below 100 K, the in-gap states dominate the nuclear relaxation at temperatures less than 10 K. The Korringa product $1/K^2T_1T$ exhibits anomalous behavior in this range and the application of high magnetic fields leads to suppression of nuclear relaxation. The hybridization gap, however, remains open up to 37 T. The behavior of the relaxation at low temperatures suggests a strong field dependence of the in-gap states and rules out the possibility that bound states arise from B_6 vacancies. A simple density-of-states model and a band scheme are introduced to account for these observations.

DOI: 10.1103/PhysRevB.75.075106 PACS number(s): 71.27.+a, 67.80.Jd, 76.60.−k

INTRODUCTION

The Kondo insulators, also known as heavy-fermion semiconductors, are stoichiometric compounds with small-gap semiconducting properties.[1,2] Most are nonmagnetic, e.g., CeNiSn, $Ce_3Bi_4Pt_3$, YbB_{12}, FeSi, and SmB_6, with a Van Vleck–like low-temperature susceptibility. The low-T resistivity and electronic specific heat follow an exponential activation law consistent with a gap in the density of states. Kondo insulators are not perfect semiconductors, because the gap is frequently only a pseudogap and/or there are intrinsic or impurity states in the band gap. In this paper, we investigate gap states in SmB_6 via high-field ^{11}B NMR.

The gap in Kondo insulators arises from the coherence of the heavy electron states at the Fermi level resulting from hybridization between the $4f$ and conduction bands. This occurs when the localized $4f$ level is close to the Fermi energy and is easily realized in cubic crystals. The hybridization gap is strongly reduced by many-body interactions (Kondo effect) and can range from 1 to 50 meV. In contrast to usual band gaps, the gap of a Kondo insulator is temperature-dependent,[3] and these materials become metallic at surprisingly low temperatures. The gap can also be gradually closed by large magnetic fields, yielding a metallic state for fields larger than a critical value.[4,5] This insulator-metal transition has been observed, for example, in the specific heat of $Ce_3Bi_4Pt_3$,[6] and can also be induced by pressure and by alloying.[7–9]

SmB_6 is an intermediate valence (IV) semiconductor where the ground state of Sm is a coherent superposition of the configurations, $4f^6$ and $4f^55d$, with weight factors 0.3 and 0.7, respectively, giving an effective $4f$ valence of 2.7. It has a small gap E_g of about 54 K determined from resistivity measurements[1,7,10] (in transport, the activation energy is $E_g/2$) and the specific heat[11] (the entropy reaches $R \ln 2$ at about 40 K). In addition, a larger gap of 155–220 K has been observed in optical reflectivity data.[12,13] Both gaps are properties of the bulk material and are believed to be a consequence of the hybridization. Similar to other Kondo insulators, such as FeSi,[14] the properties of SmB_6 can be classified using several temperature ranges. Above 50 K, the electrical conductivity is almost temperature-independent, the Hall coefficient is positive, and the material behaves like a poor metal.[15] In this range, the magnetic susceptibility is only weakly temperature-dependent.[16,17] For $6<T<50$ K, the conductivity σ is activated, the Hall coefficient is negative, and the susceptibility χ decreases slightly before reaching a roughly constant value below 20 K.[17] Below 6 K, the temperature dependence of σ is smaller, and below 2–3 K, σ is almost constant.[7] The properties below 6 K are believed to be dominated by in-gap bound states.

There is evidence for in-gap states in SmB_6 from the T dependence of the optical transmission and reflectivity through films,[12,13] light-scattering (Raman),[18] neutron-scattering experiments,[19,20] and low-T specific heat.[11] The in-gap bound states have only small spectral weight. The concentration of in-gap states is also extremely pressure-dependent, as found from high-pressure electrical resistivity and Hall-effect measurements.[7] In-gap states are also known to exist for FeSi and YbB_{12} and are thought to be a common feature in all Kondo insulators.[3,14,21,22] In-gap states can be intrinsic or arise from defects. Inherent to hexaboride crystals is a boron deficiency, which plays a significant role when the cation is divalent, e.g., for the semimetal EuB_6, the insulator CaB_6,[23] and the semiconductor SmB_6. Previous low magnetic field NMR spin-lattice relaxation measurements[17,24] suggest that the metallic Korringa-type mechanism, with allowance for a gap in the density of states, satisfactorily describes the data above 20 K. At lower temperatures, the in-gap states were not detected but it was suggested that the relaxation mechanism is due to the Wigner-crystal-like formation of localized states related to conductivity.[17] The nature of the in-gap bound states, whether intrinsic or extrinsic, is still controversial.

Several authors have proposed models for the intrinsic in-gap states. Curnoe and Kikoin suggest the existence of a singlet excitonic state, formed by a hole in the Sm ion f shell and an electron distributed over nearest-neighbor p orbitals.[25] If the binding energy of the exciton is comparable to the gap, low-lying local excitations arise. Since the in-gap states are not specific to Sm systems, but are present in other Kondo insulators (e.g., YbB_{12} and FeSi), this mechanism is not a very likely explanation for the in-gap states in SmB_6. In

a more general approach, Kasuya[26] uses a localized Kondo model to predict two different temperature regimes in SmB_6. The lowest excitation state is an *s*-wave exciton, leading to predictions consistent with neutron scattering results. Along somewhat similar lines, Riseborough has proposed that the mixed valence nature of the system gives rise to antiferromagnetic correlations leading to in-gap magnetic excitations, analogous to antiparamagnons in a metal.[22,27] It is likely that the system is close to an antiferromagnetic phase transition at low temperatures. Antiferromagnetism in Kondo insulators with bipartite lattices has previously been predicted[28] and models of field-induced transitions to a metallic phase have been considered.[29] Although these models provide explanations for various Kondo phenomena, the nature of the in-gap states in SmB_6 remains unclear.

EXPERIMENTAL

In order to provide insight into the nature of the in-gap states in SmB_6, we have carried out measurements of the ^{11}B Knight shift and spin-lattice relaxation rates on a high-purity single crystal in a wide range of applied magnetic fields. The ^{11}B-enriched $2\times2\times1$ mm^3 single crystal was grown using the aluminum flux method and was characterized using electrical resistance, x-ray diffraction, and magnetic susceptibility measurements. The residual resistance ratio is about 5000. We used a home-built pulsed NMR spectrometer that employs a quadrature phase detection scheme. Measurements of the ^{11}B spectrum and relaxation rates were carried out from 2 to 300 K over a magnetic field H ranging from 1 to 37 T provided by superconducting, resistive (Bitter), and the high-field hybrid magnet at NHMFL. The spectra were obtained by stepping the magnetic field and convoluting the Fourier transforms of the spin echoes at each field. The Knight shifts and relaxation rates were derived from the first quadrupole satellites, which distinguish between field-parallel and field-perpendicular orientations to the crystal *c* axis, as explained below. For the relaxation measurements, the spin echo was integrated and plotted as a function of variable delay after the saturation pulse. The curve is then fitted with the multiexponential recovery master equation appropriate for $|\pm3/2\rangle\leftrightarrow|\pm1/2\rangle$ transition. The small-angle tipping method was employed for high-field ($>$20 T) and low-temperature ($<$4 K) experiments, where the relaxation times were of the order of a few minutes.

RESULTS AND DISCUSSION

SmB_6 has a bcc structure with Sm ions at the corner sites and boron octahedron at the body center. When the magnetic field is applied parallel to the crystal [001] (*c* axis) direction, the ^{11}B ($I=3/2$) NMR spectrum (Fig. 1) consists of two sets of quadrupolar split components. These correspond to six equivalent boron sites whose local symmetries are noncubic. Each boron has a tetragonal symmetry along the three crystal directions such that under applied field $H\|c$, four borons (B2) lie in a plane perpendicular to H, and two (B1) lie along H (see inset). The principal axes of the electric field gradient (EFG) are along the crystal axes and the asymmetry

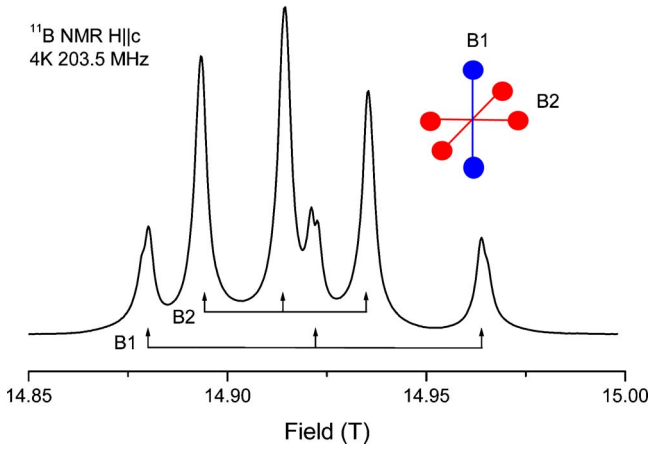

FIG. 1. (Color online) Field-swept ^{11}B NMR spectrum for field H along *c* axis (vertical) and at 4 K shows two sets (B1 and B2) of quadrupolar split lines. The just-resolved splitting of each B1 peak is due to the dipolar fields of neighboring borons along the *c* axis [001].

parameter η of the EFG vanishes in tetragonal symmetry. The first-order quadrupole shift depends on the angle θ between H and the principal axis of EFG, i.e., $\Delta\nu_{|\pm3/2\rangle\leftrightarrow|\pm1/2\rangle}\sim\frac{1}{2}\nu_Q(3\cos^2\theta-1)$ Since both the apical B1 and planar B2 nuclei are present, measurements along field directions $\theta=0°$ ($H\|c$) and $\theta=90°$ ($H\perp c$) can be obtained simultaneously in a single spectrum. We obtained a quadrupole splitting of $\nu_Q=570(3)$ kHz independent of temperature, in agreement with previous works.[17,24] However, our NMR spectra are markedly different from the early low field NMR work[17] in three aspects. First, the spectra showed a well-resolved central peak anisotropy where the $|\pm1/2\rangle\leftrightarrow|\mp1/2\rangle$ transition of the B2 sites exhibits a measureable second-order shift. Secondly, a small splitting, $\sim$12 G, of each B1 line can be distinguished, due to a nuclear dipolar coupling from neighboring borons along the *c* axis. The most important difference is that the Knight shift K derived from the spectra shows a weak but marked temperature dependence that is not observed in Ref. 17. Apart from a difference in sample quality, the application of high fields enables us to make very accurate measurements of small Knight shifts.

The Knight shift components can be related to the static susceptibility χ_o through[30–32]

$$K_i \approx \frac{A_i}{\gamma_e\gamma_n\hbar}\chi_o, \tag{1}$$

where, i=iso, ax, and γ_e and γ_n are the electron and nuclear gyromagnetic ratios, respectively. In SmB_6, the transferred hyperfine coupling A_i is dominated by the Sm ion $4f$ multiplet states.[17,33] The measured Knight shifts are shown in Fig. 2. Both the isotropic, K_{iso}, and a smaller anisotropic component K_{ax} have similar temperature behavior, as can be seen in the figure. Within experimental uncertainty, K is independent of magnetic field up to 14 T. The measured bulk magnetic susceptibility χ is also shown in Fig. 2.

For convenience in the discussion, Fig. 2 is divided into four regions, labeled I to IV. In regions I and II, where

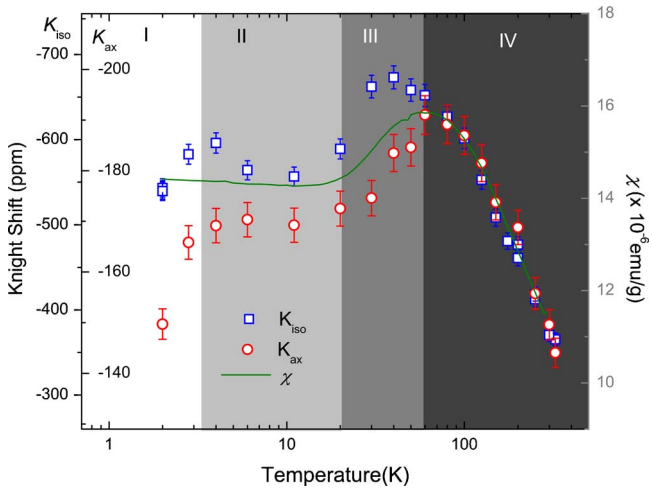

FIG. 2. (Color online) Bulk magnetic susceptibility χ and isotropic $K_{\rm iso}$ and anisotropic $K_{\rm ax}$ Knight shifts measured at 14.9 T and corrected for demagnetization effects. $K_{\rm iso}$ and $K_{\rm ax}$ scales are outside and inside the left axis, respectively. Vertical axes are scaled to match data above 60 K (region IV). The regions are described in the text.

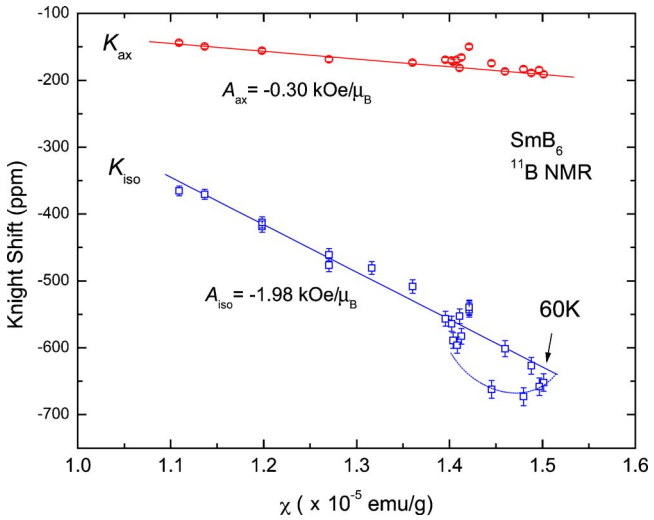

FIG. 3. (Color online) Jaccarino plot of ^{11}B Knight shift $K_{\rm ax}$ (T) vs magnetic susceptibility $\chi(T)$ for SmB_6. The breakdown in the linear correlation of K with χ for decreasing T, once the susceptibility has passed through its maximum value, is characteristic of Kondo systems.

$k_BT \ll E_g$, the susceptibility is weakly T-dependent. Below 10 K, a slight upturn in χ may be due to paramagnetic impurities. In region III the behavior arises from the thermal population of the conduction band across the gap. For region IV, $k_BT > E_g$ and the Knight shift tracks the susceptibility.

The anisotropic part of the Knight shift, $K_{\rm ax}=\frac{1}{3}(K_{\parallel}-K_{\perp})$, arises from the dipolar fields of Sm moments, while the isotropic component, $K_{\rm iso}=\frac{1}{3}(K_{\parallel}+2K_{\perp})$, comes from the transferred hyperfine fields from Sm ions through polarization of the core s electrons of the B atoms. Here, the field-parallel $K_{\parallel}$ and the field-perpendicular $K_{\perp}$ components are deduced from the average positions of the first quadrupole satellites from the B1 and B2 sites, respectively, which, in the presence of the quadrupole interaction, are unshifted in the second order. It is important to note that $K_{\rm ax}$ is very small, reflecting the fact that the moments on the Sm ions are somewhat shielded. We derive the hyperfine coupling from the slope of the Clogston-Jaccarino plot of $K(T)$ versus $\chi(T)$, with temperature as an implicit parameter shown in Fig. 3, and obtain $A_{\rm ax}=-0.30$ kOe/μ_B. In the same manner, the isotropic component is found to be $A_{\rm iso}=-1.98$ kOe/μ_B. The present value of $A_{\rm iso}$ is about twice as large as previously obtained in Ref. 17 and closer to the value deduced from their relaxation data. $A_{\rm ax}$ is correspondingly smaller by more than a factor of 2 and in better agreement with calculations, i.e., $A_{\rm ax}=-0.34$ kOe/μ_B from the lattice sum of dipolar fields from unsaturated Sm moments. The observed temperature dependence of K in the present data may account for this difference. The isotropic Pauli contribution to K is very small and positive, $K_{\rm iso}(\chi \to \chi_p) < 0.002\%$, reflecting the small carrier density in this material. Figure 3 shows that K no longer tracks χ below 60 K (regions I, II, and III) where χ decreases with decreasing T before becoming roughly constant at the lower temperatures. This behavior reflects a changeover to a new magnetic regime in which either the hyperfine coupling is no longer constant or the spin susceptibility is no longer defined by the local moments, as is expected for a hybridized state. This breakdown in the dependence of K on χ has been observed in various Kondo systems[34] and is a signature of many-body effects occurring at low temperatures.

The spin-lattice relaxation rates $(1/T_1)$ for $H \| c$ and $H \perp c$ are very similar and are shown as a function of temperature for various magnetic fields in Fig. 4. In fields up to 37 T and for $T > 20$ K, the relaxation rate is independent of field, suggesting that the gap remains open even at these high fields. This interpretation is consistent with magnetoresistance data obtained in pulsed magnetic fields.[5] Below 20 K, a field-dependent maximum in $1/T_1$ is found that persists for fields up to 13.9 T. This maximum was also previously observed in

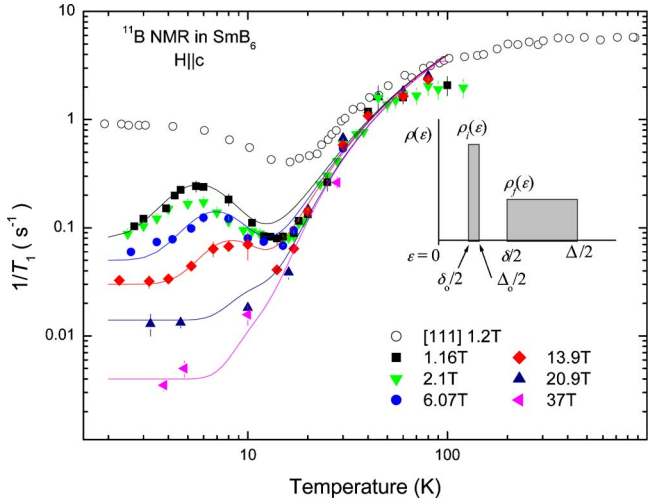

FIG. 4. (Color online) Spin-lattice relaxation rates as a function of T for different magnetic fields H. Solid curves are fit to a model density of states shown in the inset. Data at 1.2 T along [111] from Ref. 15 are shown for comparison.

Ref. 24 but not in Ref. 17. The position of this maximum shifts to higher temperatures with increasing fields, and at the highest fields the maximum is seen only as a shoulder in the relaxation rate plots. Below 5 K, $1/T_1$ shows a marked decrease with increasing H, suggesting that in regions I and II the relaxation mechanism is gradually suppressed by high fields. At the lowest temperatures (region I), the relaxation rate is essentially constant with T for a given value of H.

The fluctuating transferred hyperfine interaction between Sm $4f$ electrons and the neighboring B nuclei gives a temperature-independent relaxation rate that is inversely proportional to the spin fluctuation frequency. It has been established unequivocally that $4f$ moments fluctuating at frequencies 10^{12}–10^{13} s^{-1} account for the relaxation behavior at high temperatures (regions III and IV).[17,35] The relaxation is mainly due to states at the gap edge and thus activated, supporting the notion that the gap is a hybridization gap formed by the broad $5d$ conduction band and the narrow $4f$ band where the Fermi energy is pinned (see Fig. 5, top panel). While the high-temperature relaxation behavior is well understood, it is unclear what mechanism plays out at low temperatures. Recent nuclear forward scattering experiments have shown that under pressure (>6 MPa) when the charge gap is closed, Sm is in full trivalent state and exhibits long-range magnetic order.[36] However, without pressure there is no evidence of any magnetically ordered state down to lowest temperatures (50 mK), suggesting that the Sm moments are well shielded. It has also been argued that since the relaxation rate at low temperatures is more than two orders of magnitude slower than at high temperatures, if well-defined local moments exist at low temperatures, they would have unreasonably large fluctuating frequencies compared with the fluctuations that account for high-temperature relaxation.[17]

Analysis of the low-temperature $1/T_1$ data is complicated by the presence of the (field-dependent) maxima between 5 and 10 K. A peak in $1/T_1$ data is often associated with a critical slowing down, a crossover when the fluctuations in the hyperfine field becomes comparable to the nuclear Larmor frequency. Associated with the intermediate valence of SmB_6 are charge fluctuations that can contribute to nuclear relaxation. Valence fluctuations are frozen out at low T, but in-gap states that have been observed in numerous experiments (e.g., Refs. 13, 18, 37, and 38) could provide a relaxation mechanism for nuclear spin. Fluctuating electric-field gradients tied to charge fluctuations have previously been discounted in T_1 measurements using ^{10}B and ^{11}B probes, which show that the nuclear relaxation is purely magnetic in origin.[35]

In order to account for the data, we shall invoke a model of a narrow band of magnetic states within the gap, consistent with the other experimental results, independent of its origin. Some authors[17] have invoked the possibility of fluctuations of Sm^{3+} ions at site vacancies[24] or to localized electronic states, not associated with Sm ions, spread over several atomic distances, similar to a Wigner crystal formation.[26] Within the framework of the exciton-polaronic model, this band of states is taken to correspond to a formation of short-ranged excitons in the vicinity of Sm centers.[25] Regardless of the true origin, we see that the field dependence of the relaxation rate in the present data clearly suggests that these excitations are magnetic in nature and thus puts constraints on these various models.

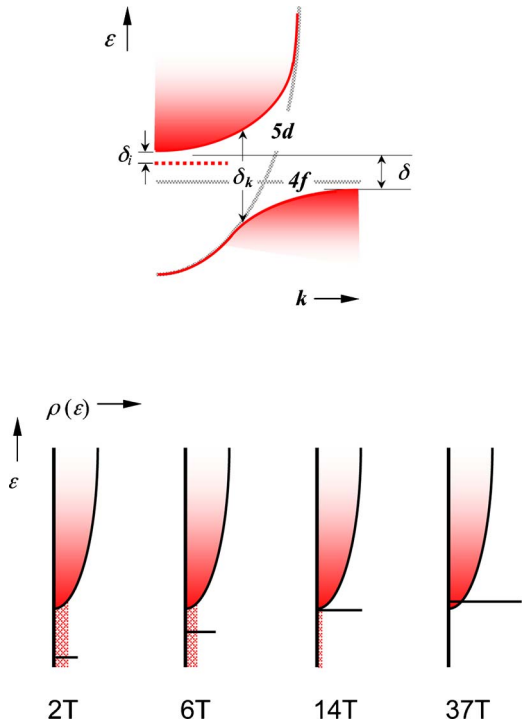

FIG. 5. (Color online) Upper panel: Insulating gap formed when a narrow $4f$ band hybridizes with a broad $5d$ band in SmB_6. Figure shows the indirect gap $\delta=V^2/D$ and the direct gap $\delta_k=V$, where V and D are the hybridization and bandwidth, respectively. The in-gap states (dotted line) are separated from the conduction band by the gap δ_i. Lower panel: Schematic representation of the relative positions of the in-gap states with respect to the conduction band as a function of magnetic field, as deduced from the T_1 data. The length of the line representing the in-gap states gives the relative amplitude of the density of states. The hatched area depicts the relative (exaggerated) residual DOS W_o suppressed by the field. The density of states for the conduction band is greatly exaggerated.

Following the standard approach, the spin-lattice relaxation rate is expressed as[30–32]

$$\frac{1}{T_1} = \frac{\hbar k_B T}{\omega_n} \sum_q A^2 F(q) \chi''_{q,\omega_n}, \tag{2}$$

with $F(q)$ being the structure factor for a particular field orientation, $\chi''_{q,\omega}$ the imaginary part of the q-dependent dynamical susceptibility, and ω_n the nuclear Larmor frequency. $\chi''_{q,\omega}$ is predominantly determined by the density of states, $\rho_f(\varepsilon)$. In regions I and II this applies to the in-gap states and at higher temperatures to the hybridized (Kondo resonance) band with the gap of diminished importance. For small ω values that are accessible in NMR experiments,

$$\chi''_{q,\omega} \approx \frac{\pi\omega}{k_B T} \int d\varepsilon\, f(\varepsilon)[1 - f(\varepsilon)]\rho_f^2(\varepsilon), \tag{3}$$

where $f(\varepsilon)$ is the Fermi distribution function. If we assume that $\rho_f(\varepsilon)$ can be represented by a Lorentzian of half-width

$\Delta/2$ centered at the Fermi level, then for $k_BT \ll \Delta$, the factor $\rho_f^2(\varepsilon)$ in Eq. (3) is approximately constant over the range of energies and can be pulled out of the integral giving $1/T_1 = \pi\hbar A^2 k_B T/\Delta^2$. For $k_BT \gg \Delta$, the Fermi function can be approximated by 1/2 over the range of integration and $1/T_1 = \pi\hbar A^2/\Delta$. Hence, the relaxation rate is Korringa-like (proportional to T) for $k_BT \ll \Delta$, while it tends to a constant value for $k_BT \gg \Delta$. We clearly see that the latter case applies well to region IV.

The data in Fig. 4 show that $1/T_1$ passes through a field-dependent maximum below 10 K. This shows that there are states within the gap that produce the observed maxima but their effects become less important as T is raised. The behavior of the maxima with field suggests that these states are field-dependent and their position moves toward the band edge as H is increased. These observations allow us to fit the data with a simple density of states (DOS) model parametrized by a hybridization gap δ. Modifying the gap model of Ref. 17, we add an extra in-gap band and assume a chemical potential μ fixed at midgap ($\varepsilon=0$) and a symmetric rectangular distribution for both the in-gap band and the conduction band for states above μ. Using these simplifying assumptions in Eqs. (2) and (3) yields

$$\frac{1}{T_1} \approx -2k_BT\left[\rho_f\left\{f\left(\frac{\Delta}{2}\right) - f\left(\frac{\delta}{2}\right)\right\} + \rho_i\left\{f\left(\frac{\Delta_o}{2}\right) - f\left(\frac{\delta_o}{2}\right)\right\}\right] + W_o, \tag{4}$$

where the band edges and the energy gaps Δ, Δ_o, δ, and δ_o are shown in the inset of Fig. 4. Here, the in-gap band is separated from the conduction band by a smaller gap $\delta_i \equiv (\delta - \Delta_o)/2$.

The results of this analysis are shown as solid lines in Fig. 4 and are fits to Eq. (4). The availability of several magnetic field data allows us to constrain the values of many fit parameters. For example, for all fields, the width of the hybridized band Δ is fixed at 800 K with the corresponding fixed uniform density of states ρ_f. The width of the in-gap band is set at $(\Delta_o - \delta_o)/2 = 5$ K but with a temperature-dependent amplitude given by $\rho_i \propto \rho_o \exp(-T/T_0)$, where $T_0 = 1.5$ K, and ρ_o is a fit parameter. The separation δ_i is allowed to be dependent on H, corresponding to field suppression of the in-gap states. In the low field limit ($H \to 0$), the value obtained, $\delta_i = 30$ K, is in excellent agreement with that obtained in Ref. 13. The fact that the maximum in the relaxation rate shifts to higher temperatures with increasing field implies that this band separation vanishes at around 14 T. Above this field, the gap $\delta = 110$ K, separating the valence from the conduction band, determines the behavior of the system. The residual low temperature DOS ($\propto W_o$) is found to be suppressed by field exponentially, $W_o \sim \exp(-H/H_c)$, with $H_c \sim 11$ T. This field-dependent W_o in region I may be formed by the tail in the density distribution not accounted for by our simplistic model and is probably linked to weak magnetic correlations that are suppressed by large fields. As the temperature is increased, the hybridized band of width Δ begins to dominate the relaxation process.

The model fits the data very well. The hybridization energy gap δ derived from the fit is twice as large as E_g and

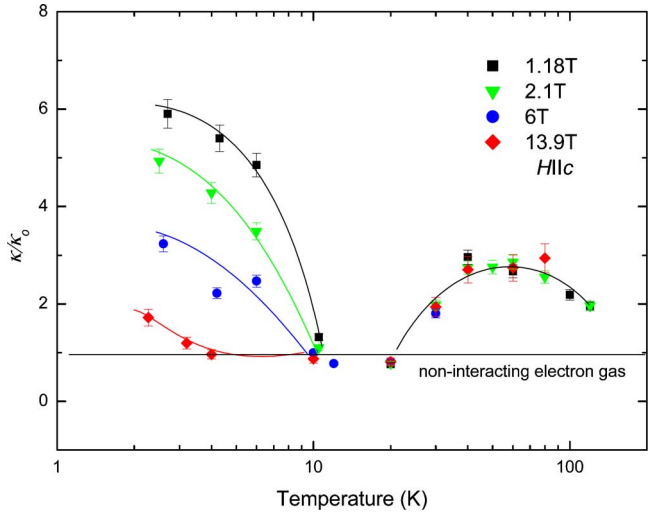

FIG. 6. (Color online) The Korringa product, $\kappa = (K_\parallel^2 T_1 T)^{-1}$, in the [001] direction, normalized using the standard Korringa constant κ_o. The horizontal line $[K(\alpha) = \kappa/\kappa_o = 1]$ represents the noninteracting electron gas value. The enhancement factor $K(\alpha)$, which allows for spin correlation effects, is discussed in the text. Lines are guides to the eye.

from previous NMR measurements[17,24] but agrees with the value obtained from conductivity data (19 meV).[13] The discrepancy could be a result of our crude approximation to the density of states $\rho(\varepsilon)$, which in reality is k-dependent, may contain Van Hove singularities, and is not necessarily symmetric about μ. Nevertheless, the qualitative predictions are not sensitive to this detail and the present model captures the essential physics of low-temperature relaxation by introducing effects due to field-dependent in-gap states. We emphasize that the insulating gap derived from high-temperature resistivity corresponds to δ. The gap δ_i is a smaller effect that is known to play a role at low temperatures and low fields. Figure 5 is a conceptual rendition of the position of the in-gap states relative to the conduction band showing the suppression of δ_i at high fields.

It is instructive to determine the enhancement in electronic correlations in SmB_6 over the free electron gas value. Figure 6 shows the Korringa product $\kappa = (K_\parallel^2 T_1 T)^{-1}$ for several field values applied along the c axis and normalized by the noninteracting Fermi gas value for ^{11}B, $\kappa_o = (\gamma_e/\gamma_n)^2 \hbar/4\pi k_B = 1.01 \times 10^{-4}$ s K. The Korringa product absorbs any temperature dependence of the hyperfine field A in Eq. (2). In terms of the enhancement factor $K(\alpha)$, where α is associated with the Stoner susceptibility factor,[39] we write $\kappa = K(\alpha)\kappa_o$. At temperatures below the Kondo temperature in the case of antiferromagnetic spin fluctuations, $K(\alpha) > 1$, resulting in enhanced values for the Korringa product. A value close to unity for the enhancement factor $K(\alpha)$ implies the usual normal metallic behavior.

Figure 6 shows that above 20 K, the enhancement factor exhibits a universal behavior that is independent of field. The $K(\alpha)$ peaks at around 60 K, concomitant with the peak in χ. Interestingly, no enhancement was found in the narrow temperature regime $\sim 10 < T < 20$ K and at high temperatures, where the data tend to approach unity. With increasing tem-

perature, excitations to the conduction band begin to build up at 20 K resulting in enhanced correlations. Below 10 K, however, $K(\alpha)$ shows a marked increase that is strongly field-dependent. The enhancement is almost completely suppressed by the 14 T field. We note that this is also the field at which the gap δ_i vanishes (Fig. 5). This suggests that the low-temperature dynamics and thus $K(\alpha)$ can be fully accounted for by the in-gap states. The enhancement due to these states decreases with temperature and its influence completely disappears at $\sim$10 K, where $K(\alpha) \rightarrow 1$, where it remains up to 20 K. That $K(\alpha)$ becoming unity in this temperature range (10–20 K) is unexpected in a highly correlated Kondo system, but it is possible that it is a manifestation of a balance between the local moment correlations and an insulating behavior in which the same correlations are suppressed. This temperature range also marks a crossover from one kind of correlated behavior defined by the in-gap states to another where the relaxation is governed by excitations across the hybridization gap. The low-temperature additional contributions to the relaxation coming from the in-gap states are strongly field- and temperature-dependent such that at higher fields, the condition $K(\alpha) \rightarrow 1$ is achieved at lower temperatures, implying that these states inherit the magnetic character due to the hybridization with the $4f$ electrons.

CONCLUSION

In summary, the Knight shifts and nuclear spin-lattice relaxation rates of the Kondo insulator system SmB_6 have been measured between 1.5 and 300 K in magnetic fields up to 37 T. The hybridization gap remains open at all fields. In examining the NMR properties, several regions are distinguished. At high T, for k_BT larger than the width of the Kondo resonance, the Knight shift behavior with T is closely linked to the static magnetic susceptibility, and $1/T_1$ is essentially constant. The range $20 < T < 60$ K exhibits exponential activation due to the gap. For $3 < T < 20$ K, field-dependent maxima in the relaxation rates are observed. Finally, at low T the relaxation rate tends to a constant value. The relaxation rate is strongly field dependent below 20 K, and essentially field independent for $T > 20$ K. The model density of states, which includes field-dependent in-gap states, fully accounts for this behavior over a wide temperature range. The Korringa product is consistent with conventional metallic-type behavior in a narrow temperature regime, and the field-dependent enhancement in this quantity below 10 K is attributed to the in-gap states.

As mentioned earlier, in-gap states can either be intrinsic or arise due to doping. For SmB_6, the latter may arise from a B_6 deficiency in the hexaborides (electron doping). Each defect can give rise to a bound state in the gap, and with sufficient concentration an impurity band can be formed, which pins the Fermi level.[40] However, an impurity band of this kind, since it arises from B_6 vacancies, should have a weak field dependence, in contrast to our observations. Intrinsic magnetic states in the gap as suggested in Ref. 27, on the other hand, arise from an exchange interaction and have a strong magnetic response. In-gap states have been observed in many experiments, including inelastic neutron scattering, Raman scattering, and optical transmission. These states are possibly responsible for the saturation of the resistivity at low T and the electronic low T specific heat. The NMR results present fresh evidence for their magnetic nature.

ACKNOWLEDGMENTS

The authors acknowledge stimulating discussions with D. MacLaughlin, S. Curnoe, M. Aronson, M. Takigawa, and S. van Molnar. The assistance of M. Abdelrazek, R. Achey, and D. Young in the early part of this work is greatly appreciated. Work performed under the auspices of NSF In-House Research Program and the State of Florida under cooperative agreement DMR-0084173. P.S. acknowledges support from DOE and NSF. Z.F. acknowledges support from NSF Grant No. DMR-0433560.

*Present address: MST-10 K764, Los Alamos National Laboratory, Los Alamos, NM 87545.
†Present address: Dept. of Physics, University of California-Davis, Davis, CA 95616.

[1] G. Aeppli and Z. Fisk, Comments Condens. Matter Phys. **16**, 155 (1992).
[2] P. Riseborough, Adv. Phys. **49**, 257 (2000).
[3] Z. Schlesinger, Z. Fisk, H. T. Zhang, M. B. Maple, J. F. DiTusa, and G. Aeppli, Phys. Rev. Lett. **71**, 1748 (1993).
[4] A. Millis, in *Physical Phenomena at High Magnetic Fields*, edited by E. Manousakis *et al.* (Addison-Wesley, Reading, MA, 1991), p. 146.
[5] J. C. Cooley, C. H. Mielke, W. L. Hults, J. D. Goettee, M. M. Honold, R. M. Modler, A. Lacerda, D. G. Rickel, and J. L. Smith, J. Supercond. **12**, 171 (1999).
[6] M. Jaime, R. Movshovich, G. R. Stewart, W. P. Beyermann, M. G. Berisso, M. F. Hundley, P. C. Canfield, and J. L. Sarrao, Nature (London) **405**, 160 (2000).
[7] J. C. Cooley, M. C. Aronson, Z. Fisk, and P. C. Canfield, Phys. Rev. Lett. **74**, 1629 (1995).
[8] J. C. Cooley, M. C. Aronson, A. Lacerda, Z. Fisk, P. C. Canfield, and R. P. Guertin, Phys. Rev. B **52**, 7322 (1995).
[9] S. Yeo, S. Nakatsuji, A. D. Bianchi, P. Schlottmann, Z. Fisk, L. Balicas, P. A. Stampe, and R. J. Kennedy, Phys. Rev. Lett. **91**, 046401 (2003).
[10] P. Wachter, in *Handbook on the Physics and Chemistry of Rare Earths*, edited by K. A. Gschneider, Jr. and L. Eyring (North-Holland, Amsterdam, 1994), Vol. 19.
[11] S. von Molnar, T. Theis, A. Benoit, A. Briggs, J. Flouquet, and J. Ravex, in *Valence Instabilities*, edited by P. Wachter and H. Boppart (North-Holland, Amsterdam, 1982), p. 389.
[12] T. Nanba, H. Ohta, M. Motokawa, S. Kimura, S. Kunii, and T. Kasuya, Physica B **186–188**, 440 (1993).
[13] B. Gorshunov, N. Sluchanko, A. Volkov, M. Dressel, G. Knebel,

A. Loidl, and S. Kunii, Phys. Rev. B **59**, 1808 (1999).
[14] N. E. Sluchanko, V. V. Glushkov, S. V. Demishev, A. A. Menovsky, L. Weckhuysen, and V. V. Moshchalkov, Phys. Rev. B **65**, 064404 (2002).
[15] J. W. Allen, B. Batlogg, and P. Wachter, Phys. Rev. B **20**, 4807 (1979).
[16] R. L. Cohen, M. Eibschütz, and K. W. West, Phys. Rev. Lett. **24**, 383 (1970).
[17] M. Takigawa, H. Yasuoka, Y. Kitaoka, T. Tanaka, H. Nozaki, and Y. Ishizawa, J. Phys. Soc. Jpn. **50**, 2525 (1981).
[18] P. Nyhus, S. L. Cooper, Z. Fisk, and J. Sarrao, Phys. Rev. B **55**, 12488 (1997).
[19] P. A. Alekseev, J.-M. Mignot, J. Rossat-Mignod, V. N. Lazukov, and I. P. Sadikov, Physica B **186–188**, 384 (1993).
[20] P. A. Alekseev, J. M. Mignot, J. Rossat-Mignod, V. N. Lazukov, I. P. Sadikov, E. S. Konovalova, and Yu B. Paderno, J. Phys.: Condens. Matter **7**, 289 (1995).
[21] A. Bouvet, T. Kasuya, M. Bonnet, L. P. Regnault, J. Rossat-Mignod, F. Iga, B. Fåk, and A. Severing, J. Phys.: Condens. Matter **10**, 5667 (1998).
[22] P. S. Riseborough, Phys. Rev. B **68**, 235213 (2003).
[23] P. Vonlanthen, E. Felder, L. Degiorgi, H. R. Ott, D. P. Young, A. D. Bianchi, and Z. Fisk, Phys. Rev. B **62**, 10076 (2000).
[24] O. Peña, M. Lysak, D. E. MacLaughlin, and Z. Fisk, Solid State Commun. **40**, 539 (1981).
[25] S. Curnoe and K. A. Kikoin, Phys. Rev. B **61**, 15714 (2000).
[26] T. Kasuya, J. Phys. Soc. Jpn. **65**, 2548 (1996).
[27] P. S. Riseborough, Ann. Phys. **9**, 813 (2000).
[28] V. Dorin and P. Schlottmann, Phys. Rev. B **46**, 10800 (1992).
[29] T. Ohashi, A. Koga, S. I. Suga, and N. Kawakami, Phys. Rev. B **70**, 245104 (2004).
[30] A. Narath, in *Hyperfine Interactions*, edited by A. Freeman and R. Frankel (Academic Press, London, 1967), p. 287.
[31] N. Bulut, D. W. Hone, D. J. Scalapino, and N. E. Bickers, Phys. Rev. B **41**, 1797 (1990).
[32] A. J. Millis, H. Monien, and D. Pines, Phys. Rev. B **42**, 167 (1990).
[33] K. Hanzawa, J. Phys. Soc. Jpn. **67**, 3151 (1998).
[34] E. Kim and D. L. Cox, Phys. Rev. B **58**, 3313 (1998).
[35] O. Peña, D. E. MacLaughlin, and M. Lysak, J. Appl. Phys. **52**, 2152 (1981).
[36] A. Barla, J. Derr, J. P. Sanchez, B. Salce, G. Lapertot, B. P. Doyle, R. Ruffer, R. Lengsdorf, M. M. Abd-Elmeguid, and J. Flouquet, Phys. Rev. Lett. **94**, 166401 (2005).
[37] N. E. Sluchanko, V. V. Glushkov, B. P. Gorshunov, S. V. Demishev, M. V. Kondrin, A. A. Pronin, A. A. Volkov, A. K. Savchenko, G. Gruner, Y. Bruynseraede, V. V. Moshchalkov, and S. Kunii, Phys. Rev. B **61**, 9906 (2000).
[38] V. V. Glushkov, A. V Kuznetsov, O. A. Churkin, S. V. Demishev, Yu. B. Paderno, N. Yu. Shitsevalova, and N. E. Sluchanko, Physica B **378**, 614 (2006).
[39] A. Narath and H. T. Weaver, Phys. Rev. **175**, 373 (1968).
[40] P. Schlottmann, J. Appl. Phys. **75**, 7044 (1994).